Excitation of gravity modes in the parameter space of the tidal wind system

S. Blanco and O.A. Rosso

Instituto de Cálculo, Facultad de Ciencias Exactas y Naturales, Universidad de Buenos Aires
Pabellón II, Ciudad Universitaria, 1428 Buenos Aires, Argentina

A. Costa and G. Domenech

Instituto de Astronomía y Física del Espacio
C.C. 67 Suc. 28, 1428 Buenos Aires, Argentina

Perturbing the Navier-Stokes equation in the ionospheric F-region, the dispersion relation and the unstable regions in wavenumber space are derived as a function of two control parameters, the colatitude θ and the slow time evolution for tidal modes τ. Our results satisfy the internal gravity wave (IGW) dispersion relation and are in good agreement with observational data. Also, we obtained a nice prediction for the excitation regions of these modes in the parameter space (θ, τ). The distribution of IGW excitations, in this parameter space is in very good agreement with observational data distributed along the day. An alternative explanation to the disappearence of IGW near the equator is given. Our model predicts an interesting latitude dependence, which needs to be tested by new observational data.

Keywords: Gravity modes; tidal wind; ionospheric F-region

En este trabajo derivamos —perturbando la ecuación de Navier-Stokes en la región F de la ionósfera— la relación de dispersión y la ubicación de regiones inestables en el espacio de número de ondas como funciones de dos parámetros de control: la colatitud θ y el tiempo lento τ de evolución. Nuestros resultados satisfacen la relación de dispersión de las ondas de gravedad internas (IGW) y acuerdan satisfactoriamente con los datos observacionales. La distribución de las excitaciones IGW en el espacio de los parámetros también acuerda con los datos distribuidos a lo largo del día. Presentamos una posible explicación a la desaparición de las IGW cerca del Ecuador. Nuestro modelo predice una dependencia interesante de los modos con la latitud que necesitaría que debería ser corroborada con nuevos datos observacionales.

Descriptores: Ondas de gravedad; mareas; región F de la ionósfera

1. Introduction

Density and velocity irregularities with periods shorter than terdiurnal tide observed at D, E and F atmospheric regions were initially attributed to turbulence [1]. However, several observed periodicities and regular characteristics have led to the belief that data variability in quasi-periodic oscillations might cause the appearance of irregularities. These features were observed at a large wind tidal scale and also at a small fluctuation scale, and were attributed by Hines [2] to the action of internal gravity waves usually present at discontinuities or due to density stratification and impulsive energy sources [3, 4]. The spectrum analysis of the perturbations was investigated by Georges [5], who identified two different types of waves: Large scale waves of horizontal velocities between 400 and 1000 m/min (with periods around 80 min to 8 hs respectively, and horizontal wave numbers of $|k_x|$, $|k_y| \sim 10^{-5}$ m^{-1}); and medium-scale waves propagating with horizontal velocities about 100–250 m/min with periods of about 15 min to 1 hs and horizontal wave number vectors $|k_x|$, $|k_y| \sim 10^{-4}$ m^{-1}. The vertical wave numbers were of about 10^{-3} m^{-1} in both cases.

More recent data of the low atmospheric F region (250–500 km) were described in the literature as the nonlinear enhancement between internal gravity waves (IGW) and the tidal wind system (TWS). Different descriptions take into account the energy transport [6], the coupling of gravity modes [7] and the induction of a thin turbulent layer due to mode coupling [8]. These papers use characteristic data for both tidal and gravitational modes.

Most studies of atmospheric structure and wave behavior were conducted, at lower altitudes, mainly at stratospheric and mesospheric heights, producing a wealth of new results in recent years. In the present paper, our aim is to apply these studies made at lower altitudes, to see if the thermosphere presents a similar behavior. Basically, we assume that slow and convective instabilities [9] have an important role to play in the upper atmosphere as they do in the lower atmosphere.

We derive a self consistent description which, taking into account the above mentioned problems, gives as a result the IGW as nonlinear perturbations of tidal modes. Nonlinear perturbative techniques describing the behavior of autonomous systems are common in the literature [10, 11]. The first step is to perform a linear analysis in terms of the free parameters. Linear instability regions can be identified in a space formed by these free parameters, usually called "control parameters", whose variation from stable to unstable linear regions, give rise to new stable nonlinear equilibria (in this context, the Hopf bifurcations play the role of internal

gravity waves). The richness of the information we could extract from this linear analysis (the excitation regions of IGW) constrained our first paper to this approximation and encouraged us to attempt a nonlinear calculation in a subsequent work.

A general description requires the calculation of the excitation regions in the parameter space; the whole set of excited modes, labelled by $\vec{k}$ and ω (the wave number and frequency respectively); the amplitude of the IGW and their relaxation times. From a complete nonlinear study the amplitudes of the IGW can be obtained as the nonlinear saturation of the linear excitation. The linear analysis gives, in terms of the control parameters θ and τ, the boundaries of the regions where the dynamics of the system changes and the characteristic $\vec{k}$ and ω of the perturbation in these boundaries. We assume that the characteristic times associated to the perturbations are $t \ll \tau$, which in turn justifies an autonomous treatment.

The paper is organized in the following way: the model, the procedure and the approximations for solving the equations are presented in Sects. 2 and 3, respectively. Section 4, is devoted to some results and discussions in connection with the previous model. Finally, in Sect. 5 we summarize our conclusions.

2. The model

There is an extensive literature devoted to the description of atmospheric tidal winds produced by gravitational and thermal effects [1, 12]. Tidal fields are described by linearizations around the steady state of the Navier-Stokes, continuity and energy balance equations of a compressible, stratified, non-adiabatic fluid, taking into account Coriolis effects, the gravitational potential due to the earth, the sun and the moon, and thermal effects as well.

Assuming the earth gravity as constant (g) and neglecting magnetohydrodynamic and viscous effects we can write

$$\frac{D\vec{v}}{Dt} = -\frac{\nabla P}{\rho} - 2\vec{\Phi} \times \vec{v} - g\hat{z} + \mathcal{F}, \qquad (1)$$

$$\frac{\partial \rho}{\partial t} + \nabla \cdot (\rho \vec{v}) = 0, \qquad (2)$$

$$\frac{DP}{Dt} - s^2 \frac{D\rho}{Dt} = (\gamma - 1)\mathcal{Q}\rho \qquad (3)$$

where $\mathcal{F}$ is the force associated to the tidal gravitational potential (sun and moon) and $\mathcal{Q}$ are the heat sources. $\vec{\Phi}$ is the earth's rotational velocity, $\gamma = C_P/C_V$, s is the sound velocity and D/Dt is the total derivative.

We assume the usual convention for the tidal functional dependence of the velocity field, density and pressure:

$$\vec{v} = [U(x,y,z,\tau), V(x,y,z,\tau), W(z,\tau)], \qquad (4.1)$$

$$\rho = \rho(z,\tau), \qquad (4.2)$$

$$P = P(z,\tau). \qquad (4.3)$$

TABLE I. Tidal amplitudes, their derivatives with respect to z, phases and periods [6, 12]. Characteristic lenghts and the Froud and Rossby numbers.

	Semidiurnal Tide	Diurnal Tide	Units
B_U	3000	4200	m/min
B_V	3000	2700	m/min
B_W	180	120	m/min
$\dfrac{\partial B_U}{\partial z}$	-0.015	-0.015	1/min
$\dfrac{\partial B_V}{\partial z}$	-0.020	-0.020	1/min
$\dfrac{\partial B_W}{\partial z}$	54×10^{-5}	54×10^{-5}	1/min
Phase	9 A.M.	7 A.M.	hrs
$T^{(T)}$	720	1440	min
$D^{(T)}$	2160	3888	km
$L^{(T)}$	130	172	km
F	10^{-3}	0.5×10^{-3}	
R_o	1	0.5	

Our aim is to obtain the IGW through the perturbation of Eqs. (1) to (3) around the steady tidal solutions, taking into account that for the IGW the atmosphere behaves as an adiabatic and incompressible stratified medium. Thus, we impose adiabaticity and incompressibility to the perturbation. Then, the IGW must satisfy $\nabla \cdot \vec{v}' = 0$ and also $P' = s^2 \rho'$ [13]. The characteristic frequency of the IGW due to stratification, the Brunt-Väisälä frequency $[N^2 = -(g/\rho)(\partial \rho/\partial z)]$, is in our case $N^2 = 1.6$ min^{-2}, which means that stratification is stable.

The z vertical background wind component (TWS) is an order of magnitude smaller than the horizontal one, so its dependence on horizontal coordinates might be neglected. Then, these dependences for W, ρ and P have been neglected in Eq. (4) [1, 6]. The values of Froude and Rossby numbers show that the stratification effects are preponderant and the relevance of the rotation effects. As $L^{(T)} \ll D^{(T)}$ (vertical vs. horizontal characteristic scale lengths), R_o, and F numbers are small enough (see Table I), the evolution of the background and perturbations can be thought of as large-scale quasi-horizontal field [13].

For the tidal fields we take an average phenomenogical solution whose functional dependence will be given below. We choose a local coordinate system where $\hat{x}$ is parallel to $\hat{\theta}$, $\hat{y}$ is parallel to $\hat{\varphi}$ and $\hat{z}$ is perpendicular to the earth surface. θ is the colatitude.

From phenomenological data [6, 14] we can conclude that the length scale $D^{(T)}$ of variation of the tidal velocity components U and V is much larger than the gravity horizontal wavelength, $D^{(G)} \sim 0.1 D^{(T)}$, then we can use a multiple scale method where $\vec{k}$ and ω are defined as local wavenum-

ber and they depend on the parameters θ and τ, where θ is the colatitude and τ, the slow time evolution for tidal modes. This means that a magnitude, *e.g.*, U can be written as $U' = U(\theta, \tau) + A_1 e^{i\varepsilon^{-1}f(\theta,\tau)}$ where $f(\theta, \tau) = k_x(\theta, \tau)x - \omega(\theta, \tau)t$ and $k_x(\theta, \tau) = \varepsilon^{-1}\partial f/\partial x$, $\omega(\theta, \tau) = \varepsilon^{-1}\partial f/\partial t$. The small parameter ε characterizes the scale separation.

In summary, in our case the linear expressions of the perturbation amplitudes $\mathbf{A}_i$ of the velocity $\vec{v}$, the density ρ and

the pressure P can be written as

$$
\begin{pmatrix} U' \\ V' \\ W' \\ \rho' \\ P' \end{pmatrix} = \begin{pmatrix} U \\ V \\ W \\ \rho \\ P \end{pmatrix} + e^{i(\vec{k}\cdot\vec{x}-\omega t)}\begin{pmatrix} \mathbf{A}_1 \\ \mathbf{A}_2 \\ \mathbf{A}_3 \\ \mathbf{A}_4 \\ \mathbf{A}_5 \end{pmatrix} \quad (5)
$$

and $\omega = \omega_R + i\omega_I$ and $\vec{k}$ are functions of the parameters θ and τ. Also, up to zero order, the amplitudes $\mathbf{A}_i$ are not time dependent.

The resulting perturbed equations are

$$
\rho\Big[i(\vec{v}\cdot\vec{k}-\omega)+\frac{\partial U}{\partial x}\Big]\mathbf{A}_1+\rho\Big(\frac{\partial U}{\partial y}-2\phi_z\Big)\mathbf{A}_2+\rho\Big(\frac{\partial U}{\partial z}+2\phi_y\Big)\mathbf{A}_3+\Big[\frac{\partial U}{\partial t}+(\vec{v}\cdot\nabla U)+2(\phi_y W-\phi_z V)\Big]\mathbf{A}_4+ik_x\mathbf{A}_5=0, \quad \text{(6.a)}
$$

$$
\rho\Big(\frac{\partial V}{\partial x}+2\phi_z\Big)\mathbf{A}_1+\rho\Big[i(\vec{v}\cdot\vec{k}-\omega)+\frac{\partial V}{\partial y}\Big]\mathbf{A}_2+\rho\Big(\frac{\partial V}{\partial z}-2\phi_x\Big)\mathbf{A}_3+\Big[\frac{\partial V}{\partial t}+(\vec{v}\cdot\nabla V)+2(\phi_z U-\phi_x W)\Big]\mathbf{A}_4+ik_y\mathbf{A}_5=0, \quad \text{(6.b)}
$$

$$
-2\rho\phi_y\mathbf{A}_1+2\rho\phi_x\mathbf{A}_2+\rho\Big[i(\vec{v}\cdot\vec{k}-\omega)+\frac{\partial W}{\partial z}\Big]\mathbf{A}_3+\Big[\frac{\partial W}{\partial t}+W\frac{\partial W}{\partial z}+2(\phi_x V-\phi_y U)+g\Big]\mathbf{A}_4+ik_z\mathbf{A}_5=0, \quad \text{(6.c)}
$$

$$
\frac{\partial \rho}{\partial z}\mathbf{A}_3+\big[i(\vec{v}\cdot\vec{k}-\omega)+(\nabla\cdot\vec{v})\big]\mathbf{A}_4=0, \quad (7)
$$

$$
s^2(\vec{v}\cdot\vec{k}-\omega)\mathbf{A}_4-(\vec{v}\cdot\vec{k}-\omega)\mathbf{A}_5=0. \quad (8)
$$

Here we have neglected the terms $\mathcal{Q}\cdot\mathbf{A}_4$ and the perturbation of the gravitational tidal force $\mathcal{F}$.

In the derivation of Eq. (7) we have explicitly used the fact that the perturbation (IGW) is incompressible, that is, $\nabla\cdot\vec{v}' = 0$. In Eq. (8) the contribution proportional to $\mathbf{A}_3$ is cancelled by virtue of the usual definition of the velocity of sound $s^2 = dP/d\rho$. Then, from this equation we recover the relation $P' = s^2\rho'$ for the perturbation.

The functional dependence of the tidal velocity field $\vec{v}$ was modeled as

$$
U(\theta, z, \tau) = \big[\mathbf{B}_U^{(d)}(z)\cos(\Omega_1\tau)
$$
$$
+ \mathbf{B}_U^{(s)}(z)\cos(\Omega_2\tau - \pi/3)\big]\cdot f_U(\theta), \quad \text{(9.a)}
$$

$$
V(\theta, z, \tau) = \big[\mathbf{B}_V^{(d)}(z)\cos(\Omega_1\tau)
$$
$$
+ \mathbf{B}_V^{(s)}(z)\cos(\Omega_2\tau - \pi/3)\big]\cdot f_V(\theta), \quad \text{(9.b)}
$$

$$
W(\theta, z, \tau) = \big[\mathbf{B}_W^{(d)}(z)\cos(\Omega_1\tau)
$$
$$
+ \mathbf{B}_W^{(s)}(z)\cos(\Omega_2\tau - \pi/3)\big]\cdot f_W(\theta) \quad \text{(9.c)}
$$

where θ is the colatitude. $f_U(\theta)$, $f_V(\theta)$ and $f_W(\theta)$ are the tidal wind colatitudinal dependence.

There are several diurnal and semidiurnal modes acting simultaneously, but at this altitude ($z \sim 300$ km) the deepest modes are the simetrical $(-1, 1)$ and $(2, 2)$ Hough modes. These modes present a rather similar colatitudinal behavior: near null at the pole and maximizing at mid and low colatitudes. For simplicity in this scenario, the same colatitudinal behavior shall be adopted for diurnal and semidiurnal modes,

TABLE II. Parameters values employed in the model [14, 16].

$\|\vec{\Phi}\|$	4.36×10^{-3}	1/min
Ω_1	4.36×10^{-3}	1/min
Ω_2	8.73×10^{-3}	1/min
s	2.6×10^3	m/min
g	32040	m/min^2
ρ	2×10^{-8}	gr/m^3
$\dfrac{\partial\rho}{\partial z}$	-10^{-12}	gr/m^4

using a colatitudinal function between 0 and 90 degrees (we use the same function for the north and south hemisphere) given by: $f_U(\theta) = f_V(\theta) = (2\theta/\pi + 1/2)\cos(\pi/4 - \theta)$ and $f_W(\theta) = 1$. A more complex colatitudinal structure at F-region is being studied, but differences due to individual modes contribution are not yet conclusive. The amplitudes $\mathbf{B}^{(d),(s)}$, as well as the phases and periods of the diurnal and semidiurnal tides respectively are shown in Table I [6, 12]. Note that due to the proportionality of $\hat{y}$ to τ, the y dependence of these expressions has been absorbed in the τ dependence. The gravity constant g, sound speed s, the density $\rho(z)$ and its derivative $\partial\rho/\partial z$ were estimated from tables [16, 17]; the amplitudes $\mathbf{B}(z)$, and their derivatives, $(\partial\mathbf{B}_U)/(\partial z)$, $(\partial\mathbf{B}_V)/(\partial z)$ and $(\partial\mathbf{B}_W)/(\partial z)$ were estimated from tables and graphics [6, 12] and are shown in Tables I and II for a height $z \cong 300$ km.

3. The procedure

The system given by Eqs. (6) to (8), has nontrivial solutions in the amplitudes $\mathbf{A}$ if its complex determinant is equal to

zero. After a long but straightforward calculation we obtained the determinant that gives two equations in ω_R and ω_I:

$$\mathbf{C}_{00} + \mathbf{C}_{01}\omega_I + \mathbf{C}_{02}\omega_I^2 + \mathbf{C}_{03}\omega_I^3 + \mathbf{C}_{04}\omega_I^4$$
$$+ \mathbf{C}_{10}\omega_R + \mathbf{C}_{11}\omega_R\omega_I + \mathbf{C}_{12}\omega_R\omega_I^2$$
$$+ \mathbf{C}_{20}\omega_R^2 + \mathbf{C}_{21}\omega_R^2\omega_I + \mathbf{C}_{22}\omega_R^2\omega_I^2$$
$$+ \mathbf{C}_{30}\omega_R^3 + \mathbf{C}_{40}\omega_R^4 = 0, \qquad (10.a)$$

$$\mathbf{D}_{00} + \mathbf{D}_{01}\omega_I + \mathbf{D}_{02}\omega_I^2 + \mathbf{D}_{03}\omega_I^3$$
$$+ \mathbf{D}_{10}\omega_R + \mathbf{D}_{11}\omega_R\omega_I + \mathbf{D}_{12}\omega_R\omega_I^2 + \mathbf{D}_{13}\omega_R\omega_I^3$$
$$+ \mathbf{D}_{20}\omega_R^2 + \mathbf{D}_{21}\omega_R^2\omega_I$$
$$+ \mathbf{D}_{30}\omega_R^3 + \mathbf{D}_{31}\omega_R^3\omega_I = 0, \qquad (10.b)$$

where the coefficients $\mathbf{C}$ and $\mathbf{D}$ (whose explicit expressions are given in Appendix I) depend on the components of the wave vector $\vec{k}$ and of the tidal model both dependent on the control parameters (θ, τ). Note, that this means that the dispersion relation, [Eqs. (10)], depends only on the control parameters. The modes that can be excited are those with $\omega_I > 0$. We obtain these excitation regions and the damping ones ($\omega_I < 0$) by looking for the set of points were $\omega_I = 0$.

The set of points that we obtained, turned out to be one dimensional curves in the (θ, τ) space. A curve that delimites two regions in the parameters space with different signs of ω_I at both sides will be the separatrix line between damping and excitation zones.

Replacing $\omega_I = 0$ in Eqs. (10.a) and (10.b) we obtain that ω_R must satisfy the following equations (dispersion relation):

$$\mathbf{C}_{00} + \mathbf{C}_{10}\omega_R + \mathbf{C}_{20}\omega_R^2 + \mathbf{C}_{30}\omega_R^3 + \mathbf{C}_{40}\omega_R^4 = 0 \quad (11.a)$$

$$\mathbf{D}_{00} + \mathbf{D}_{10}\omega_R + \mathbf{D}_{20}\omega_R^2 + \mathbf{D}_{30}\omega_R^3 = 0. \quad (11.b)$$

Since the dispersion relation is unique either Eq. (11.a) and Eq. (11.b) are the same (if $\mathbf{C}_{40}\omega_R^4$ is negligibly small) or the set of roots of Eq. (11.b) is included in the set of roots of Eq. (11.b).

If we estimate from literature ω_R and $\vec{k}$ characteristic values of the IGW and using the TWS parameters [5, 6, 14], we notice that, for the extreme values of $\omega_R \sim 10^{-2}$ min^{-1} and $4\vec{v} \cdot \vec{k} \sim 10^{-2}$ min^{-1} there is an order of magnitude of difference between $\mathbf{C}_{40}\omega_R^4$ and $\mathbf{C}_{30}\omega_R^3$. In the average case this relation gives a difference of two or three orders of magnitude. Then we can say that $\mathbf{C}_{40}\omega_R^4 \ll \mathbf{C}_{30}\omega_R^3$. If we repeat the same procedure for the other terms, we found that $\mathbf{C}_{20}/(\omega_R\mathbf{C}_{30}) < 10^3$. This allows us to neglect the term $\mathbf{C}_{40}\omega_R^4$ in Eq. (11.a) and consider that Eq. (11.a) and Eq. (11.b) are the same term by term. From this assumption we were able to determine a functional form (denoted by f) for the set of points (θ_b, τ_b) in the parameter space (θ, τ) that satisfy the condition $\omega_I = 0$ and the associated wave vector $\vec{k}(\theta, \tau)$ in selfconsistent way.

Note that the consistency of the method will be proved if the resulting values satisfy the hypothesis of the model

(about the autonomous condition and the local wave number) and the inequality estimated previously from phenomenological values (from the predicted values of the model given in Table III, we have: $\omega_R \sim 510^{-3}$ min^{-1}; $v \sim \lambda/T \sim 10^{-2}$ m/min; $k_z \sim 10^{-3}$ m^{-1} then $\mathbf{C}_{40}\omega_R^4$ is less than two order of magnitude than $\mathbf{C}_{30}\omega_R^3$).

Then

$$f^{(0)}(\theta_b, \tau_b) + \xi\Delta f(\theta_b, \tau_b) = 0, \qquad (12)$$

$$k_x = k_x^{(0)}(\theta_b, \tau_b) + \xi\Delta k_x(\theta_b, \tau_b), \qquad (13.a)$$

$$k_y = k_y^{(0)}(\theta_b, \tau_b) + \xi\Delta k_y(\theta_b, \tau_b), \qquad (13.b)$$

$$k_z = k_z^{(0)}(\theta_b, \tau_b) + \xi\Delta k_z(\theta_b, \tau_b); \qquad (13.c)$$

where

$$\xi = \rho\left[s^2\frac{\partial\rho}{\partial z}\right]^{-1} = \left(-\frac{g}{s^2}\right)\frac{1}{N^2}, \qquad (14)$$

$$f^{(0)} = \left(\vec{k}^{(0)} \cdot \vec{v}\right) + (\nabla \cdot \vec{v})/2, \qquad (15)$$

$$\Delta f = \Delta k_x U + \Delta k_y V + \Delta k_z W \qquad (16)$$

explicit expressions of which are given in Appendix II.

In Eqs. (12) and (13) the term with parameter ξ is proportional to the stratification of the medium. The parameter ξ is related to the Brunt-Väisälä frequency N [13]. In our model, for the reference height $z \cong 300$ km, $\xi \cong -2.910^{-3}$ min^2/m corresponding to a Brunt-Väisälä frequency of about $N \cong 1.2$ min^{-1}.

The solution of Eq. (12) gives the boundary values (θ_b, τ_b) in the parameter space where $\omega_I(\theta_b, \tau_b) \cong 0$ and they are shown in Fig. 1. These curves, which prove to separate the damping and excitation regions (the signs of ω_I at both side of the curve are different), are the separatrix lines. With the limiting values given in Fig. 1 we evaluated the corresponding values of $\vec{k}$ using Eqs. (13.a)–(13.c).

The $\vec{k}$ values are solutions of Eqs. (11.a) and (11.b) with $\omega_I = 0$. The corresponding values of $\vec{k}$ out of these curves are unknown but close to the boundaries they must coincide with the values previously obtained. Moreover, near the separatrix lines, the $\vec{k}$ values must be continuous and cannot be too different from the set obtained before. Then, for the parameter values $\theta \approx \theta_b$ and $\tau \approx \tau_b$ we can assume $\vec{k}(\theta, \tau) \approx \vec{k}(\theta_b, \tau_b)$ and $\omega_R(\theta, \tau) \approx \omega(\theta_b, \tau_b)$ and solve Eqs. (10.a) or (10.b) to obtain ω_I near the borders, outside the separatrix lines. The sign of $\omega_I(+/-)$ indicates respectively the growth or damping of the perturbation in each region. The corresponding results are symbolized with plus and minus signs in Fig. 1.

4. Results and discussion

Following the procedure described in the previous section we obtain characteristic values $k_x \sim 10^{-5}$ m^{-1}, $k_y \sim 10^{-4}$ m^{-1} and k_z with a rather steady value, $k_z \sim 5 \cdot 10^{-3}$ m^{-1} and periods T between 100 and 200 min (see Table III).

TABLE III. Characteristic values for $\theta = 40°$ and $z = 300$ km in the separatrix lines S_i of $\vec{k}$ [m^{-1}], ω_R [min^{-1}] and their respectives λ [m] and T [min]. Note that for S_4 the two crossing values are given.

|	S_1	S_2	S_3	S_4	S_5	S_6	S_7
k_x	-3.69×10^{-5}	1.16×10^{-5}	3.97×10^{-5}	2.39×10^{-5} 1.21×10^{-5}	-2.14×10^{-5}	1.24×10^{-5}	-4.83×10^{-5}
k_y	-2.73×10^{-4}	3.91×10^{-3}	-3.59×10^{-4}	-1.12×10^{-3} -7.70×10^{-4}	1.62×10^{-3}	4.25×10^{-4}	-2.92×10^{-3}
k_z	5.66×10^{-3}	5.66×10^{-3}	5.67×10^{-3}	5.66×10^{-3} 5.66×10^{-3}	5.66×10^{-3}	5.67×10^{-3}	5.66×10^{-3}
$\omega_R^{(1)}$	6.46×10^{-3}	9.70×10^{-3}	6.43×10^{-3}	5.69×10^{-3} 5.95×10^{-3}	7.69×10^{-3}	6.16×10^{-3}	4.34×10^{-3}
$\omega_R^{(2)}$	-8.10×10^{-3}	-5.82×10^{-3}	-5.70×10^{-3}	-6.75×10^{-3} -6.71×10^{-3}	-5.99×10^{-3}	-6.21×10^{-3}	-7.35×10^{-3}
λ_x	2.71×10^{4}	8.62×10^{4}	2.51×10^{4}	4.18×10^{4} 8.26×10^{4}	4.67×10^{4}	8.06×10^{4}	2.07×10^{4}
λ_y	3.66×10^{3}	2.55×10^{2}	2.78×10^{3}	8.92×10^{2} 1.29×10^{3}	6.17×10^{2}	2.35×10^{3}	3.42×10^{2}
λ_z	1.76×10^{2}	1.76×10^{2}	1.76×10^{2}	1.76×10^{2} 1.76×10^{2}	1.76×10^{2}	1.76×10^{2}	1.76×10^{2}
$T^{(1)}$	154	103	155	175 168	130	162	230
$T^{(2)}$	123	171	175	148 149	166	161	136
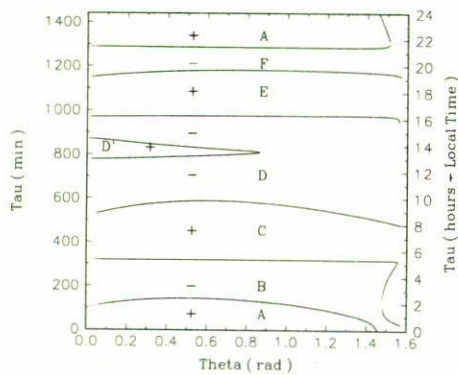
FIGURE 1. Excitation and damping regions for the IGW as a function of θ and τ, A, C and E (sign +) denote excitation zones. B, D, D' and F (sign −) denote damping zones.

FIGURE 2. Experimental values of spectral power density in the range 10–90 minutes obtained at: ■ Buenos Aires, ○ Tucumán and $\triangle$, $\triangledown$ San Juan. A, C and E denote excitation zones. B, D, D' and F denote damping zones (see Fig. 1).

In Table III we present the $\vec{k}$ values with their corresponding wave length λ, the frequencies ω_R and the corresponding periods T on the separatrix lines for $\theta = 40°$ and $z = 300$ km. The set of third solutions of Eq. (11), $\omega_R^{(3)} \approx 10^3$ m^{-1}, are not shown because the associated periods range out of the scale of validity of the model. We stress that all values of Table III correspond to the separatrix lines and not to the effective zones of excitation or damping. This values are in very good agreement with George's spectrum analysis [5] whose values were given in the Introduction.
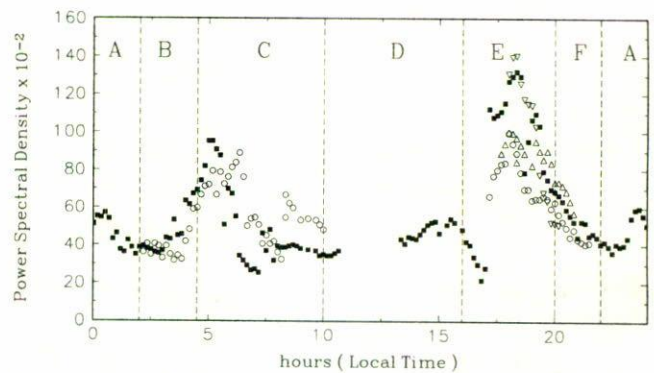
Figure 1 displays the excitation and damping regions for the IGW as function of parameters θ and τ. At different hours during the day, instabilities appear superimposed to the tidal wind signal, which are identified as IGW [6, 14]. This is confirmed by the observational data given in Fig. 2 [6] where the spectral power density of the background wind field *versus* local time is shown.

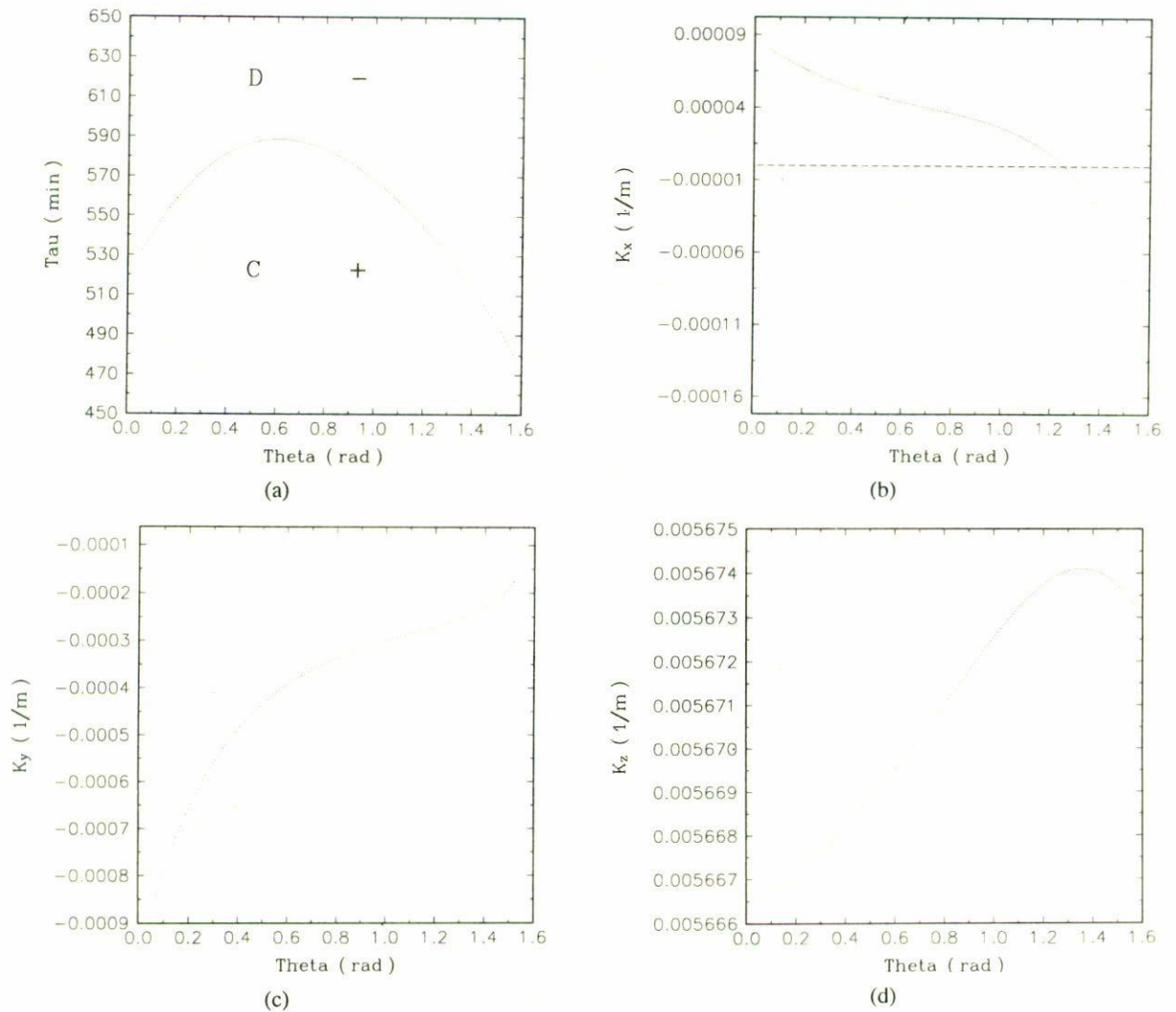We can see that there is a one-to-one correspondence among the excitation zones denoted by A, C and E in Figs. 1

FIGURE 3. a) Separatrix line (S_3) between the excitation zone C and the damping D one, in the parameter space; b) k_x values in the separatrix line S_3 vs. the colatitude; c) The same as in b for k_y; d) The same as in b for k_z.

and 2. Also, the damping zones denoted in both figures by B, D and F, show the same agreement. In Fig. 2 we can also see a latitude dependence of the data, but as their colatitude values (Buenos Aires $\theta = 0.96$ rad, Tucumán $\theta = 1.10$ rad and San Juan $\theta = 1.03$ rad) are so close, we are unable to check the complete latitude dependence. A dataset more widely spread in latitude is necessary to compare our predictions and to determine the existence of the excitation zone D' of Fig. 1.

Observational data [18] in the literature report the phenomenon of disappearence of the IGW for some hours and large colatitude values. This is generally attributed to an absorption mechanism in the medium. Our results show that $|k_x|$ and $|k_y|$ have a decreasing value as colatitude increases. Moreover, in some cases, k_x presents a change of sign for colatitudes around 75°. As an example, in Figs. 3a–3d we show this behavior for the values in the separatrix line between C and D regions. Therefore, these results provide an alternative explanation to the phenomenon of disappearence

of the IGW. Either wave reflection or the increase of excited wavelengths beyond the range of the window search can also be associated to this phenomenon. The detection of reflected waves or modes that have a strong change of λ with latitude could provide some support to this hypotesis. The data analysis of the latitude dependence and the derivation of the wave amplitudes will guide our subsequent work.

5. Conclusions

The Navier-Stokes, continuity and energy balance equations for an inviscid compressible fluid in the low atmospheric F-region were perturbed around the tidal phenomenological solution. We imposed adiabaticity and incompressibility to the perturbation. We obtained characteristic $\vec{k}$ and ω values. These modes satisfy the dispersion relation of the internal gravity waves and are in good agreement with the perturbation spectrum analysis given by Georges [5].

We derived the linear damping and excitation regions of IGW, in the parameter space of our model. In the separatrix lines (lines between excitation and damping zone of IGW) we derived in a systematic way, the wave number $\vec{k}$ and frequencies ω. They present a functional dependence with latitude θ and the slow time evolution of the tidal modes τ. The predicted time dependence of $\vec{k}$ and ω are in very good agreement with model predictions of Giraldez et al. [6] and Canciani [14] and are confirmed by experimental data given in Fig. 2.

We report an interesting behavior of the horizontal components of wavevector $\vec{k}$ near the equator line. This result is in agreement with well established observational data that report the disappearance of IGW at large colatitudes. Our model offers an alternative explanation to this disappearance, which is either wave reflection or the increase of wavelengths beyond the detection window.

We can summarize the advantages of our treatment as follows:

We obtained the IGW characteristics in a natural way from the linear analysis of the excitation modes in the system.

These characteristics (regions and boundary values of $\vec{k}$ and ω) are displayed in the free parameters space, allowing a global description of the behavior of the system. As a final remark note that a nonlinear perturbative calculation of the coupling of these modes requires the knowledge of this global description as a starting point.

Acknowledgments

Appendix I

The coefficients $\mathbf{C}$ of Eq. (7.a) are:

$$\mathbf{C}_{00} = \frac{\partial \rho}{\partial z}\left\{\alpha_1(\vec{v}\cdot\vec{k})^2 + s^2(\vec{v}\cdot\vec{k})(k_z\eta_2 - 2k_y\phi_x) + \alpha_2\beta + 2\delta\phi_x - 4\alpha_3\phi_z + 2\alpha_2\eta_1\phi_z - 2(2\nu_2 + \gamma\phi_x)W\right\}$$
$$+ \rho\left\{(\vec{v}\cdot\vec{k})^4 - (\nabla\cdot\vec{v})\left[(\beta + 2\eta_1\phi_z)\frac{\partial W}{\partial z} - 2(2\nu_2 + \gamma\phi_x)\right] - (\vec{v}\cdot\vec{k})^2\left[(\nabla\cdot\vec{v})^2 + \frac{\partial W}{\partial z}\eta_2 - 2\left(\frac{\partial V}{\partial z}\phi_x + \eta_1\phi_z\right) - \beta + 4\Phi^2\right]\right\}$$

$$\mathbf{C}_{01} = \frac{\partial \rho}{\partial z}\left\{2k_z s^2(\vec{v}\cdot\vec{k}) + 2\phi_x(\mu + 2\varphi) - \alpha_1\eta_2\right\}$$
$$+ \rho\left\{(\nabla\cdot\vec{v})\left[-6(\vec{v}\cdot\vec{k})^2 + \frac{\partial W}{\partial z}\eta_2 - 2\frac{\partial V}{\partial z}\phi_x - \beta - 2\eta_1\phi_z + 4\Phi^2\right] - (\beta + 2\eta_1\phi_z)\frac{\partial W}{\partial z} + 4\nu_2 + 2\gamma\phi_x\right\}$$

$$\mathbf{C}_{02} = -\alpha_1\frac{\partial \rho}{\partial z} + \rho\left\{(\nabla\cdot\vec{v})^2 - 6(\vec{v}\cdot\vec{k})^2 + \frac{\partial W}{\partial z}\eta_2 - 2\left(\frac{\partial V}{\partial z}\phi_x + \eta_1\phi_z\right) - \beta + 4\Phi^2\right\}$$

$$\mathbf{C}_{03} = 2\rho(\nabla\cdot\vec{v})$$

$$\mathbf{C}_{04} = \rho$$

$$\mathbf{C}_{10} = \frac{\partial \rho}{\partial z}\left\{-2\alpha_1(\vec{v}\cdot\vec{k}) - s^2(k_z\eta_2 - 2k_y\phi_x)\right\} + \rho\left\{2(\vec{v}\cdot\vec{k})\left[(\nabla\cdot\vec{v})^2 - 2(\vec{v}\cdot\vec{k})^2 + \frac{\partial W}{\partial z}\eta_2 - 2\frac{\partial V}{\partial z}\phi_x - 2\eta_1\phi_z - \beta + 4\Phi^2\right]\right\}$$

$$\mathbf{C}_{11} = -2k_z s^2\frac{\partial \rho}{\partial z} + 12\rho(\vec{v}\cdot\vec{k})(\nabla\cdot\vec{v})$$

$$\mathbf{C}_{12} = 12\rho(\vec{v}\cdot\vec{k})$$

$$\mathbf{C}_{20} = \alpha_1\frac{\partial \rho}{\partial z} + \rho\left\{6(\vec{v}\cdot\vec{k})^2 - (\nabla\cdot\vec{v})^2 - \frac{\partial W}{\partial z}\eta_2 + 2\frac{\partial V}{\partial z}\phi_x + 2\eta_1\phi_z + \beta - 4\Phi^2\right\}$$

$$\mathbf{C}_{21} = -6\rho(\nabla\cdot\vec{v})$$

$$\mathbf{C}_{22} = -6\rho$$

$$\mathbf{C}_{30} = -4\rho(\vec{v}\cdot\vec{k})$$

$$\mathbf{C}_{40} = \rho$$

and the coefficients $\mathbf{D}$ of Eq. (7.b) are:

$$\mathbf{D}_{00} = \frac{\partial \rho}{\partial z}\left\{2k_y s^2 \phi_x \frac{\partial U}{\partial x} - 2k_x s^2 \phi_x \left(\frac{\partial V}{\partial x} + 2\phi_z\right) + k_z s^2 \left[(\vec{v}\cdot\vec{k})^2 + 2\left(\eta_1 - 2\phi_z\right)\phi_z + \beta\right] + (\vec{v}\cdot\vec{k})\left[2\phi_x\left(\mu + 2\varphi\right) - \alpha_1 \eta_2\right]\right\}$$
$$+ \rho(\vec{v}\cdot\vec{k})\left\{(\nabla\cdot\vec{v})\left[-2(\vec{v}\cdot\vec{k})^2 + \frac{\partial W}{\partial z}\eta_2 - 2\frac{\partial V}{\partial z}\phi_x - 2\eta_1\phi_z - \beta + 4\Phi^2\right] - (2\eta_1\phi_z + \beta)\frac{\partial W}{\partial z} + 4\nu_2 + 2\gamma\phi_x\right\}$$

$$\mathbf{D}_{01} = \frac{\partial \rho}{\partial z}\left\{-2\alpha_1(\vec{v}\cdot\vec{k}) - k_z s^2 \eta_2 + 2k_y s^2 \phi_x\right\} + \rho\left\{2(\vec{v}\cdot\vec{k})\left[(\nabla\cdot\vec{v})^2 - 2(\vec{v}\cdot\vec{k})^2 + \frac{\partial W}{\partial z}\eta_2 - 2\frac{\partial V}{\partial z}\phi_x - 2\eta_1\phi_z - \beta + 4\Phi^2\right]\right\}$$

$$\mathbf{D}_{02} = -k_z s^2 \frac{\partial \rho}{\partial z} + 6\rho(\vec{v}\cdot\vec{k})(\nabla\cdot\vec{v})$$

$$\mathbf{D}_{03} = 4\rho(\vec{v}\cdot\vec{k})$$

$$\mathbf{D}_{10} = \frac{\partial \rho}{\partial z}\left\{-2k_z s^2(\vec{v}\cdot\vec{k}) + \alpha_1 \eta_2 - 2\phi_x\left(\mu + 2\varphi\right)\right\}$$
$$+ \rho\left\{(\nabla\cdot\vec{v})\left[6(\vec{v}\cdot\vec{k})^2 - \frac{\partial W}{\partial z}\eta_2 + 2\frac{\partial V}{\partial z}\phi_x + 2\eta_1\phi_z + \beta - 4\Phi^2\right] + \frac{\partial W}{\partial z}\left[\beta + 2\left(\eta_1 - 2\phi_z\right)\phi_z\right] - 2\left(\gamma + 2\nu_1\right)\phi_x\right\}$$

$$\mathbf{D}_{11} = 2\alpha_1 \frac{\partial \rho}{\partial z} + 2\rho\left\{6(\vec{v}\cdot\vec{k})^2 - (\nabla\cdot\vec{v})^2 - \frac{\partial W}{\partial z}\eta_2 + 2\left(\frac{\partial V}{\partial z}\phi_x + \eta_1\phi_z\right) + \beta - 4\Phi^2\right\}$$

$$\mathbf{D}_{12} = -6\rho(\nabla\cdot\vec{v})$$

$$\mathbf{D}_{13} = -4\rho$$

$$\mathbf{D}_{20} = k_z s^2 \frac{\partial \rho}{\partial z} - 6\rho(\vec{v}\cdot\vec{k})(\nabla\cdot\vec{v})$$

$$\mathbf{D}_{21} = -12\rho(\vec{v}\cdot\vec{k})$$

$$\mathbf{D}_{30} = 2\rho(\nabla\cdot\vec{v})$$

$$\mathbf{D}_{31} = 4\rho$$

where

$$\alpha_1 = g + 2\phi_x V + \frac{\partial W}{\partial t} + \frac{\partial W}{\partial z}$$

$$\alpha_2 = g + \frac{\partial W}{\partial t} + \frac{\partial W}{\partial z}W$$

$$\alpha_3 = \frac{\partial U}{\partial t}\phi_x + \left(g + \frac{\partial W}{\partial t}\right)\phi_z$$

$$\beta = \frac{\partial U}{\partial y}\frac{\partial V}{\partial x} - \frac{\partial U}{\partial x}\frac{\partial V}{\partial y}$$

$$\gamma = \frac{\partial U}{\partial z}\frac{\partial V}{\partial x} - \frac{\partial U}{\partial x}\frac{\partial V}{\partial z}$$

$$\delta = \frac{\partial U}{\partial x}\frac{\partial V}{\partial t} - \frac{\partial U}{\partial t}\frac{\partial V}{\partial x}$$

$$\eta_1 = \frac{\partial U}{\partial y} - \frac{\partial V}{\partial x}$$

$$\eta_2 = \frac{\partial U}{\partial x} + \frac{\partial V}{\partial y}$$

$$\nu_1 = \frac{\partial U}{\partial x}\phi_x + \frac{\partial U}{\partial z}\phi_z$$

$$\nu_2 = \frac{\partial U}{\partial x}\phi_x^2 + \frac{\partial U}{\partial z}\phi_x\phi_z + \frac{\partial W}{\partial z}\phi_z^2$$

$$\mu = (\vec{v}\cdot\nabla V) + \frac{\partial V}{\partial t}$$

$$\varphi = \phi_z U - \phi_x W$$

Appendix II

$$k_x^{(0)} = \left\{\phi_x\left(\beta V - \delta\right) + \phi_z\left(2\alpha_3 - 2\alpha_1\phi_z + 2\eta_1\phi_x V\right) + \frac{\partial U}{\partial x}\left[\alpha_1\eta_2 - \phi_x\left(\mu + 2\varphi\right)\right] + \left(2\nu_2 + \gamma\phi_x\right)W\right\}\left\{s^2\phi_x\left(\frac{\partial V}{\partial x} + 2\phi_z\right)\right\}^{-1}$$

$$k_y^{(0)} = \left\{\alpha_1\eta_2 - \phi_x\left(\mu + 2\varphi\right)\right\} \times \left\{s^2\phi_x\right\}^{-1}$$

$$k_z^{(0)} = \alpha_1 s^{-2}$$

$$\Delta k_x = \left\{\Delta_1\left[\beta - \frac{1}{4}(\nabla\cdot\vec{v})^2 + \frac{\partial U}{\partial x}\left(\nabla\cdot\vec{v} + \eta_2\right) + 2\left(\eta_1 - 2\phi_z\right)\phi_z\right] + \Delta_2\left[\frac{1}{20}(\nabla\cdot\vec{v}) - \frac{\partial U}{\partial x}\right] - \Delta_3\right\}\left\{2\phi_x\left(\frac{\partial V}{\partial x} + 2\phi_z\right)\right\}^{-1}$$

$$\Delta k_y = \{\Delta_1 \left(\nabla \cdot \vec{v} + \eta_2 \right) - \Delta_2\} \{2\phi_x\}^{-1}$$

$$\Delta k_z = \Delta_1$$

where

$$\Delta_1 = -\frac{5}{2}(\nabla \cdot \vec{v})^2 - \frac{\partial W}{\partial z}\eta_2 + 2\frac{\partial V}{\partial z}\phi_x + 2\eta_1\phi_z + \beta - 4\Phi^2$$

$$\Delta_2 = -2(\nabla \cdot \vec{v})^3 + 2\left(\gamma + 2\nu_1\right)\phi_x - \frac{\partial W}{\partial z}\left[\beta + 2\left(\eta_1 - 2\phi_z\right)\phi_z\right]$$

$$\Delta_3 = -\frac{7}{16}(\nabla \cdot \vec{v})^4 + \frac{1}{4}(\nabla \cdot \vec{v})^2\left[\frac{\partial W}{\partial z}\eta_2 - 2\frac{\partial V}{\partial z}\phi_x - 2\eta_1\phi_z - \beta + 4\Phi^2\right] + \frac{3}{2}(\nabla \cdot \vec{v})\left[4\nu_2 + 2\gamma\phi_x - \frac{\partial W}{\partial z}\left(\beta + 2\eta_1\phi_z\right)\right]$$

1. S. Chapman and R. Lindzen, *Atmospheric Tides*, (Gordon and Breach Science Pub. Dordrecht, Holland, 1970) p. 106.

2. C.O. Hines, *Canad. J. Phys.* **38** (1960) 1441.

3. N. Richmond, Li Yuan, and D. Fritts, *J. Atmos. Sci.* **46** (1989) 2562.

4. M.J. Buonsanto, *J. Geoph. Res.* **96** (1991) 3711.

5. T.M. Georges, *J. Atmos. Terr. Phys.* **30** (1968) 735.

6. A. Giraldez, U. Boldes, and J. Colman, *Lat. Am. Applied Res.* **19** (1989) 125.

7. T. Van Zandt and D. Fritts, *Pageoph.* **130** (1989) 110.

8. C. Sidi and J. Teitelbaum, *Atmos. Terr. Phys.* **40** (1978) 529.

9. E. Dewan and R. Good, *J. Geophys. Res.* **91** (1986) 2742.

10. G. Iooss and D. Joseph, *Elementaly Stability and Bifurcation Theory*, (Berlin-Springer, 1980) p. 123.

11. A. Costa, D. Gomez, and C. Ferro Fontan, *Ap. J.* **373** (1991) 237.

12. S. Kato, *Dynamic of the upper atmosphere*, (Reidel Publishing Co., Dordrech, 1980) p. 108.

13. M. Lesieur, *Turbulence in Fluids*, (Kluwer Academic Publishers, Dordrech, 1990) p. 40, p. 80.

14. P. Canciani, Ph.D. Tesis. Universidad de Buenos Aires, Argentina, 1991 p. 73.

15. *Handbook of Chemistry and Physics*, (The Chemical Rubber Company., Boca Raton, F114, 1969).

16. *Handbook of Chemistry and Physics*, (The Chemical Rubber Company., Boca Raton, F114, 1969).

17. *U.S. Standard Atmosphere*, (NASA, 1976) p. 15, p. 69.

18. Kyoto Symposium on Thermospheric Physic, Set 1973, *J. Atmos. Terr. Phys.* **36** (1974) 1841, 2037.